Carbon-13 Chemical Shift Tensors for Acylium Ions: A Combined Solid State NMR and Ab Initio Molecular Orbital Study

Teng Xu,[†] Dewey H. Barich,[†] Paul D. Torres,[†] John B. Nicholas,*[,‡] and James F. Haw*[,†]

Contribution from the Laboratory for Magnetic Resonance and Molecular Science, Department of Chemistry, Texas A&M University, College Station, Texas 77843, and Environmental Molecular Sciences Laboratory, Pacific Northwest National Laboratory, Richland, Washington 99352

Received August 21, 1996[⊗]

Abstract: We report the principal components of the ^{13}C chemical shift tensors for seven acylium ions, determined by both slow speed magic angle spinning (MAS) nuclear magnetic resonance (NMR) and theoretical methods. Experimentally, the acylium ions were prepared either by direct reaction of the parent acyl halides with metal halide powders, including frozen antimony pentafluoride, or by the reaction of alkyl halides with carbon monoxide on aluminum chloride ($AlCl_3$). The generalization of our recent observation of the acetylium ion on $AlCl_3$ to other cations is direct proof of free acylium ion intermediates in Friedel−Crafts acylation reactions. ^{13}C CP MAS NMR spectra of the acylium ions were acquired at temperatures ranging from 83 to 298 K, and the principal components of the ^{13}C chemical shift tensors were extracted by fitting the side band intensities of the MAS spectra. With the exception of the chloroacetylium ion, the acylium ions studied have isotropic $^{13}C_1$ chemical shifts of 154 ± 1 ppm, but clear variations in the principal components of the shift tensors were measured. The carbenium carbons of the acetylium and 2,2-dimethylpropionylium ions have axially symmetric ^{13}C chemical shift tensors, consistent with the molecular symmetry (C_{3v}), while the chemical shift tensors of the other cations were characterized by non-zero asymmetry parameters. The observation of appreciably smaller chemical shift anisotropies for C_1 in the benzoylium ions versus the values for the corresponding carbon in the alkanoyl cations is consistent with charge delocalization into the ring substituent. Additional information on the acylium cations is provided by theoretical calculations. We optimized the geometries of the acylium ions using second-order Møller-Plesset perturbation theory (MP2) and the 6-311G* basis set. We then calculated the NMR data at the MP2 level using the gauge-including atomic orbital (GIAO) method and the double-ζ (dz) and triple-ζ polarized (tzp) basis sets of Horn and Ahlrichs. While the isotropic shifts calculated at the GIAO-RHF/tzp/dz level were in error by as much as 26 ppm, the GIAO-MP2 values were in excellent agreement with the experimental measurements, as were those for most of the principal components. The calculations were also used to determine the orientations of the principal components. The results of analysis of the MP2 wave functions help answer long standing questions regarding the structure and bonding of acylium cations.

Introduction

Friedel−Crafts acylation reactions are generally believed to involve acylium ion ($[RCO]^+$) intermediates, generated by the interaction of acyl halides with Lewis acids such as $AlCl_3$.[1,2] Several acylium ions have been isolated as the crystalline salts of strong Lewis acids.[3−7] Examples include the crystal structure determinations of $[CH_3CO]^+[SbF_6]^-$ by Boer[3] and [*p*-CH_3-C_6H_6-$CO]^+[SbCl_6]^-$ by Le Carpentier.[4] Additional evidence for acylium ion intermediates is provided by infrared and nuclear magnetic resonance (NMR) studies in solution phases.[8] Akhrem et al. reported a solid state NMR study of a stoichiometric salt of $[CH_3CO]^+[AlCl_4]^-$.[9] We recently reported the principal components of the ^{13}C NMR shift tensor for the acetylium ion ($[CH_3CO]^+$ (**1**) in Figure 1), prepared by the direct adsorption of acetyl chloride onto anhydrous aluminum chloride powder.[10]

Here we extend our previous study to include six additional acylium ions (Figures 1 and 2), and present both experimental and theoretical ^{13}C NMR chemical shift tensors for all species. The generalization of our earlier observation of **1** on $AlCl_3$ to a number of other acylium ions on various Lewis acids convincingly demonstrates the existence of the cations, and strongly suggests that these cations are intermediates in Friedel−Crafts acylation reactions under these experimental conditions. As before, several cations were prepared from the acyl halides, but we also synthesized two acylium ions by the reaction of alkyl halides with CO on $AlCl_3$ or $AlBr_3$, a novel example of the Koch−Haaf reaction.[11]

* Authors to whom correspondence should be addressed.
[†] Texas A&M University.
[‡] Pacific Northwest National Laboratory.
[⊗] Abstract published in *Advance ACS Abstracts,* December 15, 1996.

(1) Olah, G. A. *Friedel−Crafts and Related Reactions*; Olah, G. A., Ed.; Wiley & Sons: New York, 1963−1965; Vols. I−IV.
(2) Olah, G. A. *Friedel−Crafts Reactions*; Olah, G. A., Ed.; Wiley & Sons: New York, 1973.
(3) Boer, F. P. *J. Am. Chem. Soc.* **1966**, *88*, 1572−1574.
(4) Chevrier, B.; Le Carpentier, J. M.; Weiss, R. *J. Am. Chem. Soc.* **1972**, *94*, 5718−5723.
(5) Le Carpentier, J.; Weiss, R. *Acta Crystallogr.* **1972**, *B28*, 1421−1429.
(6) Le Carpentier, J.; Weiss, R. *Acta Crystallogr.* **1972**, *B28*, 1430−1437.
(7) Chevrier, P. B.; Carpentier, J. L.; Weiss, R. *Acta Crystallogr.* **1972**, *B28*, 2673−2677.
(8) Olah, G. A.; Germain, A.; White, A. M. In Wiley & Sons: New York, 1976; Vol. V.
(9) Akhrem, I. S.; Orlinkov, A. V.; Bakhmutov, V. I.; Petrovskii, P. V.; Pekhk, T. I.; Lippman, A. E. T.; Vol'pin, M. E. *Dokl. Akad. Nauk SSSR* **1985**, *284*, 627−631.
(10) Xu, T.; Torres, P. D.; Beck, L. W.; Haw, J. F. *J. Am. Chem. Soc.* **1995**, *117*, 8027−8028.

S0002-7863(96)02944-7 CCC: $14.00

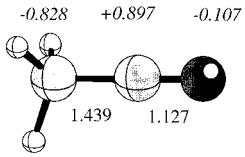

1. acetylium ion (C_{3v})

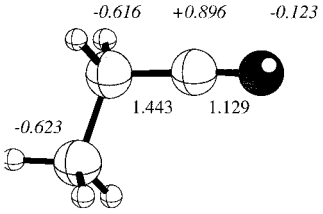

2. propionylium ion (C_s)

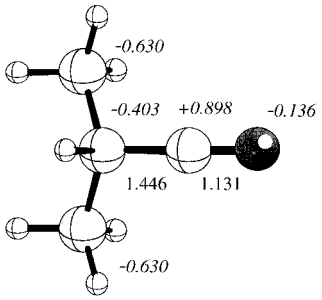

3. 2-methylpropionylium ion (C_s)

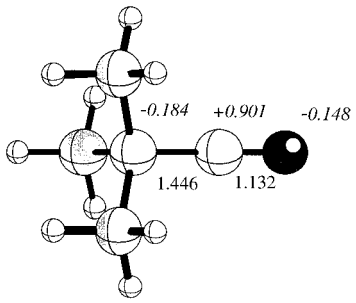

4. 2,2-dimethylpropionylium ion (C_{3v})

Figure 1. Acylium ions **1**−**4**. Selected bond lengths (plain text, in Å) and NPA partial charges (italics, in |e|) are from MP2/6-311G* optimizations.

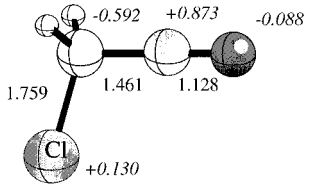

5. chloroacetylium ion (C_s)

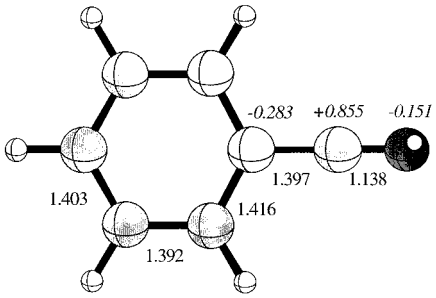

6. benzoylium ion (C_{2v})

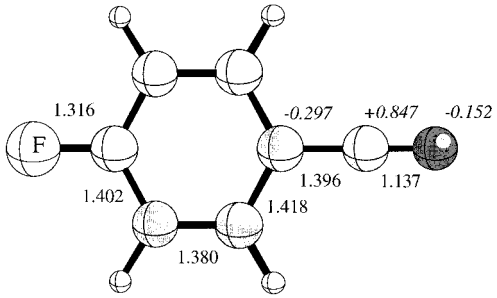

7. *p*-fluorobenzoylium ion (C_{2v})

Figure 2. Acylium ions **5**−**7**. Selected bond lengths (plain text, in Å) and NPA partial charges (italics, in |e|) are from MP2/6-311G* optimizations.

We obtain additional insight into the experimental data via ab initio molecular orbital theory, which gives the optimized geometries of the acylium ions, a detailed picture of their electronic structure, and in particular, their ^{13}C chemical shift tensors. The theoretical calculations also allow us to determine the orientation of the chemical shift tensor in the molecular frame of reference. The principal components of the ^{13}C chemical shift tensors have been reported for only a few carbenium ions,[12−16] and this report more than doubles that number. The demonstrated very good agreement between experimental and calculated tensor components is strong verification of both approaches. In addition, this work indicates that good agreement between the theoretical prediction and the experimental shift components of the acylium ions does not require the inclusion of Lewis acid counteranions in the theoretical model, as was necessary for the isopropyl cation.[17] The theoretical geometries of the cations are in good agreement with previous crystallographic studies. We also obtain theoretical estimates of the influence of possible resonance structures, which were previously discussed in a qualitative manner.[4,7]

Background

NMR chemical shifts provide valuable information about molecular structure and bonding.[18] While the determination of reliable shift data has long been solely the domain of the experimentalist, recent improvements in theoretical methodology now allow the routine calculation of magnetic properties, in particular the chemical shift tensor. Early attempts at the theoretical determination of chemical shifts were hampered by computational expense and the problem of gauge dependence common to all magnetic phenomena. The idea of using gauge-including atomic orbitals (GIAOs, also known as London orbitals), which have a formal dependence on magnetic field strength and thereby circumvent the gauge origin problem, was first implemented at the ab initio Hartree−Fock level by

(11) Koch, H.; Haaf, W. *Ann* **1958**, *618*, 251−266.
(12) Yannoni, C. S. *Acc. Chem. Res.* **1982**, *15*, 201−208.
(13) Strub, H.; Beeler, A. J.; Grant, D. M.; Michl, J.; Cutts, P. W.; Zilm, K. W. *J. Am. Chem. Soc.* **1983**, *105*, 3333−3334.
(14) Xu, T.; Haw, J. F. *J. Am. Chem. Soc.* **1994**, *116*, 7753−7759.
(15) Xu, T.; Haw, J. F. *J. Am. Chem. Soc.* **1994**, *116*, 10188−10194.
(16) Arduengo, J. A.; Dixon, D. A.; Kumashiro, K. K.; Lee, C.; Power, W. P.; Zilm, K. W. *J. Am. Chem. Soc* **1994**, *116*, 6361−6367.
(17) Nicholas, J. B.; Xu, T.; Barich, D. H.; Torres, P. D.; Haw, J. F. *J. Am. Chem. Soc.* **1996**, *118*, 4202−4203.
(18) Ernst, R. R.; Bodenhausen, G.; Wokaun, A. *Principles of Magnetic Resonance in One and Two Dimensions*; Oxford Press: London, 1987.

Ditchfield in 1974.[19] In 1990, Wolinski, Hinton, and Pulay reformulated the GIAO approach in terms of analytic derivative techniques[20] making NMR calculations at the restricted Hartree−Fock (RHF) level much more tractable. Reliable theoretical NMR calculations are now possible using a variety of methods, including the IGLO (individual gauge for localized orbitals),[21−24] LORG (localized orbitals, local origin),[25−27] and GIAO[19,20] approaches. Unfortunately, neglect of electron correlation has been shown to lead to potentially large errors in the calculated isotropic chemical shifts for molecules with triple bonds, such as CO and acetonitrile.[28] Furthermore, it has recently been shown that isotropic chemical shift calculations at the GIAO-RHF level are unreliable for benzenium[29] and related carbenium ions.[16] Considering that the acylium ions studied here combine the pathological characteristics of both triple bond and carbenium ion character, the accurate calculation of the individual components of their ^{13}C chemical shift tensors is a challenging test of theory.

As pointed out in the literature[30] electron correlation can enter the calculation of the NMR data in two ways: through the *indirect* effects of electron correlation on the geometry of the molecules under study, and through the *direct* effect of inclusion of electron correlation in the calculation of magnetic properties. Gauss recently extended the GIAO approach to include dynamical electron correlation via second-order Møller-Plesset perturbation theory (GIAO-MP2).[31] Chemical shift calculations at the GIAO-MP2 level with suitably large basis sets significantly improve the calculated isotropic chemical shifts of neutral molecules with triple bonds and the benzenium ion as referenced above. Gauss has since extended the GIAO formalism to the MP3 and SDQ-MP4 levels,[32] and with Stanton, to the coupled cluster singles and doubles (CCSD) level.[33] Methods that include dynamical correlation via density functional theory (DFT) have also been developed. These include the GIAO-DFT[34−36] and SOS-IGLO-DFT[37,38] methods as well as IGLO-DFT and LORG-DFT implementations.[16] The effects of static electron correlation with multi-configurational self-consistent field (IGLO-MCSCF[39] and GIAO-MCSCF[40]) wave functions have also been studied.

Most theoretical investigations, like experimental applications of NMR, have focused on the determination of *isotropic chemical shifts* and the interpretation of these data in terms of molecular topology and bonding. However, the familiar isotropic shift is one third the trace of a second rank *chemical shift tensor* that contains up to nine unique components. The antisymmetric part of this tensor does not affect the Zeeman energy to first order,[41] and only the remaining six components are potential observables in NMR spectra. Three components of the chemical shift tensor can be measured from spectra of randomly oriented powders, and the utility of ^{13}C principal component measurements was apparent from the early work of Waugh and Pines.[42] Experimental determination of all six components of the chemical shift tensor requires that rotation plots of the spectra of a single crystal be obtained in a goniometer probe. Knowledge of the six components allows one to identify the three Euler angles necessary to orient the principal axes of the chemical shift tensor in the molecular coordinate system. While theoretical calculations naturally give all the tensor components, the determination of tensor orientation by experimental methods is less routine. It is obvious that the chemical shift tensor is much more sensitive to structure and bonding than the isotropic value. This proves true for the acylium ions studied here; *the near identical isotropic $^{13}C_1$ shifts belie large variations in the full tensors*.

In this work we combine results from both experimental and theoretical studies. The utility of the combined theoretical/experimental approach is already evident in the literature. For example, as an alternative to single crystal studies, Grant and co-workers have used methods such as magic angle hopping[43] or magic angle turning[44] experiments to obtain resolved powder patterns for polycrystalline solids with up to several dozen chemically or crystallographically distinct carbon sites. They augmented the experimentally determined principal component data with tensor orientations calculated by ab initio methods.[45−49] Grant also used the combined theoretical/experimental approach to study the ^{13}C and ^{15}N spectra of neutral aromatic molecules,[50] and in some cases the methodology reveals structural nonequivalence too subtle to be apparent in previous diffraction studies.[51] We have recently combined the use of theoretical and experimental approaches in the study of Hammett bases on zeolites,[52] H/D exchange in benzene adsorbed on a zeolite,[53] and the study of the isopropyl cation on SbF_5,[17] as summarized in a recent account.[54]

(19) Ditchfield, R. *Mol. Phys.* **1974**, *27*, 789−807.
(20) Wolinski, K.; Hinton, J. F.; Pulay, P. *J. Am. Chem. Soc.* **1990**, *112*, 8251−8260.
(21) Kutzelnigg, W. *Isr. J. Chem.* **1980**, *19*, 193.
(22) Kutzelnigg, W. *J. Mol. Struct. Theochem.* **1989**, *202*, 11−61.
(23) Kutzelnigg, W.; Fleischer, U.; Schindler, M. In Diehl, P., Fluck, E., Günther, H., Kosfeld, R., Seelig, J., Eds.; Springer-Verlag: Berlin, 1991, pp 165.
(24) Schindler, M.; Kuttzelnigg, W. *J. Chem. Phys.* **1982**, *76*, 1919−1933.
(25) Hansen, A. E.; Bouman, T. D. *J. Chem. Phys.* **1985**, *82*, 5035−5047.
(26) Hansen, A. E.; Bouman, T. D. *J. Chem. Phys.* **1989**, *91*, 3552−3560.
(27) Bouman, T. D.; Hansen, A. E. *Chem. Phys. Lett.* **1990**, *175*, 292.
(28) Gauss, J. *J. Chem. Phys.* **1993**, *99*, 3629−3643.
(29) Sieber, S.; Schleyer, P. v. R.; Gauss, J. *J. Am. Chem. Soc.* **1993**, *115*, 6987−6988.
(30) Bühl, M.; Gauss, J.; Hofmann, M.; Schleyer, P. v. R. *J. Am. Chem. Soc.* **1993**, *115*, 12385−12390.
(31) Gauss, J. *Chem. Phys. Lett.* **1992**, *191*, 614−620.
(32) Gauss, J. *Chem. Phys. Lett.* **1994**, *229*, 198−203.
(33) Gauss, J.; Stanton, J. F. *J. Chem. Phys.* **1995**, *103*, 3561−3577.
(34) Cheeseman, J. R.; Trucks, G. W.; Keith, T. A.; Frisch, M. J. *J. Chem. Phys.* **1996**, *104*, 5497−5509.
(35) Rauhut, G.; Puyear, S.; Wolinski, K.; Pulay, P. *J. Phys. Chem.* **1996**, *100*, 6310−6316.
(36) Lee, A. M.; Handy, C.; Cowell, S. M. *J. Chem. Phys.* **1995**, *103*, 10095−10109.
(37) Malkin, V. G.; Malkina, O. L.; Eriksson, L. A.; Casida, M. E.; Salahub, D. R. *J. Am. Chem. Soc.* **1994**, *116*, 5898−5908.
(38) Schreckenbach, G.; Ziegler, T. *J. Phys. Chem.* **1995**, *99*, 606−611.
(39) van Wullen, C.; Kutzelnigg, W. *Chem. Phys. Lett.* **1993**, *205*, 563−571.
(40) Ruud, K.; Helgaker, T.; Kobayashi, R.; Jorgensen, P.; Bak, K. L.; Jensen, H. J. A. *J. Chem. Phys.* **1994**, *100*, 8178−8185.
(41) Haeberlen, U. *High Resolution NMR in Solids*; Academic Press: New York, 1976.
(42) Pines, A.; Gibby, M. G.; Waugh, J. S. *Chem. Phys. Lett.* **1972**, *15*, 373−376.
(43) Hu, J. Z.; Alderman, D. W.; Ye, C.; Pugmire, R. J.; Grant, D. M. *J. Magn. Reson.* **1993**, *105A*, 82−87.
(44) Hu, J. Z.; Wang, W.; Liu, F.; Solum, M. S.; Alderman, D. W.; Pugmire, R. J.; Grant, D. M. *J. Magn. Reson.* **1995**, *113A*, 210−222.
(45) Iuliucci, R. J.; Facelli, J. C.; Alderman, D. W.; Grant, D. M. *J. Am. Chem. Soc.* **1995**, *117*, 2336−2343.
(46) Liu, F.; Phung, C. G.; Alderman, D. W.; Grant, D. M. *J. Am. Chem. Soc.* **1995**, *117*, 9323−9328.
(47) Soderquist, A.; Facelli, J. C.; Horton, W. J.; Grant, D. M. *J. Am. Chem. Soc.* **1995**, *117*, 8441−8446.
(48) Wang, W.; Phung, C. G.; Alderman, D. W.; Pugmire, R. J.; Grant, D. M. *J. Am. Chem. Soc.* **1995**, *117*, 11984−11988.
(49) Orendt, A. M.; Facelli, J. C.; Radziszewski, J. G.; Horton, W. J.; Grant, D. M.; Michl, J. *J. Am. Chem. Soc.* **1996**, *118*, 846−852.
(50) Anderson-Altmann, K. L.; Phung, C. G.; Mavromoustakos, S.; Zheng, Z.; Facelli, J. C.; Poulter, C. D.; Grant, D. M. *J. Phys. Chem.* **1995**, *99*, 10454−10458.
(51) Facelli, J. C.; Grant, D. M. *Nature* **1993**, *365*, 325−327.
(52) Nicholas, J. B.; Haw, J. F.; Beck, L. W.; Krawietz, T. R.; Ferguson, D. B. *J. Am. Chem. Soc.* **1995**, *117*, 12350−12351.
(53) Beck, L. W.; Xu, T.; Nicholas, J. B.; Haw, J. F. *J. Am. Chem. Soc.* **1995**, *117*, 11594−11595.

Experimental Details

Materials. Aluminum chloride (99.99%), aluminum bromide (99.99+%), tantalum(V) chloride (99.99%), 2-chloro-2-methylpropane (99%), 2-bromopropane (99+%), and 4-fluorobenzoyl-*carbonyl*-^{13}C chloride were obtained from Aldrich. Acetyl-*1*-^{13}C chloride and ^{13}CO were obtained from Cambridge Isotope. Propionyl-*1*-^{13}C chloride, chloroacetyl-*1*-^{13}C chloride, benzoyl-α-^{13}C chloride, 2-chloro-2-methylpropane-*2*-^{13}C, and 2-bromopropane-*2*-^{13}C were acquired from Isotec. ^{13}C enrichment in the labeled compounds was 99% or greater. All reagents were used without further purification.

Sample Preparation for MAS NMR. The CAVERN device for sample preparation is described in detail elsewhere.[55] A typical procedure was as follows: 0.3−1.0 g of metal halide powder was loaded into a 7.5-mm zirconia rotor inside a drybox under nitrogen atmosphere; the rotor was placed into the CAVERN device, attached to the vacuum line, and evacuated to a final pressure of less than 10^{-4} Torr. For liquid SbF_5 samples, several freeze−pump−thaw cycles were applied instead of evacuation at room temperature. Gas-phase/solid phase reactions of acyl halides with metal halide powders or frozen SbF_5 were typically done at 223 K using a loading of ca. 0.15 equiv (molecules per Lewis site). We followed this experimental preparation procedure for the acetylium (**1**), propionylium (**2**), and 2-chloroacetylium ions (**5**). For the benzoylium (**6**) and *p*-fluorobenzoylium ions (**7**), the vapor pressures of their acyl halide precursors are too low to permit the direct gas-phase/solid-phase reactions. Therefore, **6** and **7** were prepared by mixing 0.2 equiv of acyl chlorides with SbF_5 in a zirconia rotor inside a drybox, and the sample was subjected to several freeze−pump−thaw cycles. 2-Methylpropionylium ion (**3**) and 2,2-dimethylpropionylium ion (**4**) were prepared by reacting carbon monoxide with 2-chloropropane and 2-chloro-2-methylpropane, respectively. Specifically, 0.2 equiv of alkyl halide was first reacted with $AlCl_3$ or $AlBr_3$ for ca. 20 min, and the sample was then exposed to ca. 600 Torr of ^{13}CO for about 40 min at 223 K. The rotor was then capped at the adsorption temperature or lower and transferred to a precooled NMR probe.

NMR Spectroscopy. ^{13}C NMR experiments were performed on a modified Chemagnetics CMX-300 MHz spectrometer operating at 75.36 MHz. We used hexamethylbenzene (17.4 ppm for the methyl carbons) as the external chemical shift standard. Chemical shift parameters are reported relative to tetramethylsilane (TMS). Chemagnetics-style pencil probes spun 7.5 mm zirconia rotors at 1 to 6.5 kHz with active spin speed control (±3 Hz).

A number of NMR experiments were performed at different temperatures, including the following: cross polarization[56] (CP, contact time = 2 ms, pulse delay = 1−30 s, 800−2000 transients); cross polarization with interrupted decoupling[57] (contact time = 2 ms, pulse delay = 1 s, 800−2000 transients, dipolar dephasing time of 50 μs); and single pulse excitation (Bloch decay) with proton decoupling or without proton decoupling (pulse delay = 4−100 s, 200 transients).

The principal components of the ^{13}C chemical shift tensors for the acylium ions were extracted by fitting the side band intensities of the ^{13}C CP MAS spectra using the Herzfeld−Berger algorithm.[58] The sample rotation speeds were set so as to provide at least three orders of spinning side bands, and in most cases five orders of side bands were acquired. The peak amplitudes were used in the Herzfeld−Berger analysis.

We define the principal values of the chemical shift tensor as $\delta_{11} \geq \delta_{22} \geq \delta_{33}$. The isotropic shift ($\delta_{iso}$) is the average of the three principal components, i.e.,

$$\delta_{iso} = {}^1/_3(\delta_{11} + \delta_{22} + \delta_{33})$$

The asymmetry factor (η) and chemical shift anisotropy (CSA) are defined by the following equations to conform with the convention found in a text by Duncan,[59] which is similar to conventions found in Harris[60] and Fyfe.[61]

For $|\delta_{11} - \delta_{iso}| \geq |\delta_{33} - \delta_{iso}|$,

$$\mathrm{CSA} = {}^3/_2(\delta_{11} - \delta_{iso})$$

$$\eta = (\delta_{22} - \delta_{33})/(\delta_{11} - \delta_{iso})$$

For $|\delta_{11} - \delta_{iso}| \leq |\delta_{33} - \delta_{iso}|$,

$$\mathrm{CSA} = {}^3/_2(\delta_{33} - \delta_{iso})$$

$$\eta = (\delta_{22} - \delta_{11})/(\delta_{33} - \delta_{iso})$$

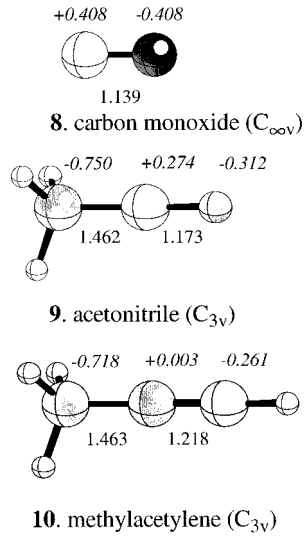

8. carbon monoxide ($C_{\infty v}$)

9. acetonitrile (C_{3v})

10. methylacetylene (C_{3v})

Figure 3. Molecules **8**−**10**. Selected bond lengths (plain text, in Å) and NPA partial charges (italics, in |e|) are from MP2/6-311G* optimizations.

Theoretical Details

Ab initio molecular orbital techniques were used to study the seven acylium ions (Figures 1 and 2). Also included are carbon monoxide (**8**), acetonitrile (**9**), and methylacetylene (**10**) (Figure 3), the geometry and electronic structure of which we will compare to those of the acylium ions. We fully optimized **1**−**10** using the analytical gradient techniques within the program Gaussian 94.[62] Low levels of theory (typically restricted Hartree−Fock (RHF) with 3-21G* basis sets) were used for the initial determination of the geometries. The final results we report here were obtained using the 6-311G* basis set[63] and electron correlation at the second order Møller−Plesset perturbation theory (MP2) level.[64] The core electrons were frozen in the MP2 calculations. We allowed the molecules complete flexibility during the geometry optimizations except for reasonable symmetry constraints, as indicated in Figures 1−3. The ^{13}C chemical shift data were calculated at the MP2 level using the GIAO formalism and the MP2/6-311G* geometries. In the GIAO-MP2 calculations we represented all hydrogens

(54) Haw, J. F.; Nicholas, J. B.; Xu, T.; Beck, L. W.; Ferguson, D. B. *Acc. Chem. Res.* **1996**, *29*, 259−267.
(55) Munson, E. J.; Ferguson, D. B.; Kheir, A. A.; Haw, J. F. *J. Catal.* **1992**, *136*, 504−509.
(56) Pines, A.; Gibby, M. G.; Waugh, J. S. *J. Chem. Phys.* **1973**, *59*, 569−590.
(57) Opella, S. J.; Frey, M. H. *J. Am. Chem. Soc.* **1979**, *101*, 5854−5856.
(58) Herzfeld, J.; Berger, A. E. *J. Chem. Phys.* **1980**, *73*, 6021−6030.
(59) Duncan, T. M. *A Compilation of Chemical Shift Anisotropies*; The Farragut Press: Chicago, 1990.
(60) Harris, R. K. *Nuclear Magnetic Resonance Spectroscopy*; Wiley & Sons: New York, 1989.
(61) Fyfe, C. A. *Solid State NMR for Chemists*; C.F.C. Press: Ontario, 1983.
(62) Gaussian 94, Revision B.1; Frisch, M. J.; Trucks, G. W.; Schlegel, H. B.; Gill, P. M. W.; Johnson, B. G.; Robb, M. A.; Cheeseman, J. R.; Keith, T.; Petersson, G. A.; Montgomery, J. A.; Raghavachari, K.; Al-Laham, M. A.; Zakrzewski, V. G.; Ortiz, J. V.; Foresman, J. B.; Cioslowski, J.; Stefanov, B. B.; Nanayakkara, A.; Challacombe, M.; Peng, C. Y.; Ayala, P. Y.; Chen, W.; Wong, M. W.; Andres, J. L.; Replogle, E. S.; Gomperts, R.; Martin, R. L.; Fox, D. J.; Binkley, J. S.; Defrees, D. J.; Baker, J.; Stewart, J. P.; Head-Gordon, M.; Gonzalez, C.; Pople, J. A.; Gaussian, Inc.: Pittsburgh, PA, 1995.
(63) Hehre, W. J.; Radom, L.; Schleyer, P.; Pople, J. A. *Ab Initio Molecular Orbital Theory*; Wiley: New York, 1986.
(64) Møller, C.; Plesset, M. S. *Phys. Rev.* **1934**, *46*, 618−622.

by double-ζ (dz) and all heavy atoms by triple-ζ polarized (tzp) basis sets of Schäfer et al.[65] The contractions are (4s/2s) for H, (9s5p1d/5s3p1d) for C, O, N, and F, and (12s9p1d/7s5p1d) for Cl. Six d-functions were used in the GIAO calculations. Schleyer et al.[29] have demonstrated that a similar scheme−combining optimizations at the MP2/6-31G* level with GIAO-MP2/tzp/dz NMR calculations−gives good agreement with experimental values for a variety of cations. For molecules **1** and **8**−**10**, GIAO-RHF calculations were done with the 6-31G*, 6-311G*, and tzp/dz basis sets to demonstrate the effect of basis set flexibility and electron correlation on the theoretical NMR values. We used the program ACES II for the GIAO-RHF and GIAO-MP2 chemical shift calculations.[66] Chemical shift data are given relative to the values for carbon in TMS, calculated at the same level of theory.

Because the antisymmetric contribution to the tensor is not observed in the experiment (vide supra), some mathematical treatment of the calculated output is required. To compare the calculated chemical shift tensors with experimental values, we first averaged the upper and lower triangles of the tensors, then diagonalized the symmetrized tensor to obtain the principal components. A program that takes chemical shift tensor data from quantum chemistry codes, calculates principal components and CSA values, and creates output for visualization of the molecules with superimposed tensor orientation is available from the authors.[67]

We analyzed the MP2/6-311G* wave functions of each molecule using the Natural Bond Orbital (NBO), Natural Population Analysis (NPA), and Natural Resonance Theory (NRT) methods.[68,69] Natural Bond Orbitals are a strongly localized, orthogonal set of bonding orbitals that have the property that a minimal basis of NBOs is guaranteed to recover more of the total electron density than any other minimal basis. That is, NBOs have maximum one- and two-center occupancy. The NBO analysis allows us to describe the electronic structure in terms of s and p bonds and lone pairs (n), and corresponding antibonding (s*, p*, and n*) and Rydberg-type (r*) orbitals. As the name implies, NPA gives estimates of the partial charges on atomic centers. These values are generally much less basis set dependent than those from the more common Mulliken population analysis.[70,71] While the partial atomic charge is not quantum-mechanically defined, the NPA provides estimates that relate well to the traditional concepts of charge polarization in organic chemistry. Similarly, NRT provides estimates of the contribution of various possible resonance (Lewis) structures to the overall resonance hybrid.

Experimental Results

Preparation of Acylium Ions. In a recent communication, several of us reported the preparation of **1** by the adsorption of acetyl chloride onto anhydrous $AlCl_3$ powder at room temperature. We have in addition made this cation from the acetyl chloride on anhydrous $AlBr_3$, $TaCl_5$, and SbF_5. In the case of SbF_5, all adsorptions and reactions were carried out at temperatures well below 280 K, the freezing point of the pure acid.

Figure 4 reports representative spectra of cation **1** and compares the principal components of the ^{13}C chemical shift tensor of C_1 measured from spinning and non-spinning spectra on two Lewis superacids ($TaCl_5$ and SbF_5). Figures 4a and 4b show ^{13}C spectra acquired at 298 K of a sample prepared by adsorption of acetyl-*1*-^{13}C chloride on $TaCl_5$. In this case, acetyl-*1*-^{13}C chloride was converted to cation **1** (153 ppm peak)- and a donor−acceptor complex with the oxygen of acetyl halide

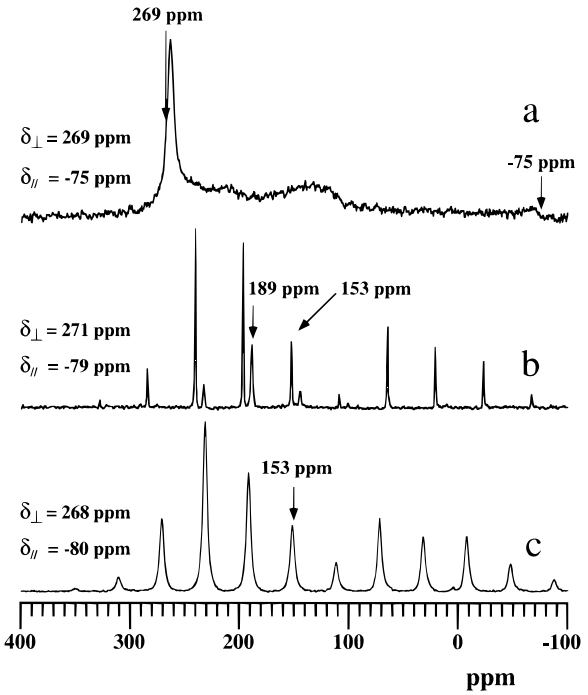

Figure 4. 75.35-MHz ^{13}C CP spectra of acetylium ion (**1**) on $TaCl_5$ (a and b) and on frozen SbF_5 (c). Spectra (a) and (b) were acquired at 298 K with a 10 s pulse delay. (a) Non-spinning spectrum, 4000 scans; (b) MAS spectrum, 200 scans; (c) MAS spectrum acquired at 83 K, the average of 2000 scans with a pulse delay of 1 s. See text for details.

(189 ppm). A quantitative Bloch decay spectrum of this sample (spectrum not shown) indicates that ca. 80% of the reactant was converted to cation **1**. An analogous donor−acceptor complex between acetyl chloride and $AlCl_3$ was also observed in our previous communication,[10] and at least one crystal structure has been reported for such a complex.[3] The non-spinning ^{13}C spectrum acquired on $TaCl_5$ at 298 K (Figure 4a) is dominated by the very broad powder pattern due to the orientation dependence of the chemical shift of **1**. The two unique principal components for this axially symmetric cation were estimated from the inflection points. As expected, the slow speed MAS spectrum in Figure 4b affords greatly improved signal to noise, even with far fewer transients. This spectrum shows two well resolved side-band patterns centered on the isotropic peak for cation **1** at 153 ppm and the donor−acceptor complex at 189 ppm. The principal components of the chemical shift tensor were calculated for **1** from MAS spectra by analyzing the side-band intensities using the numerical procedure of Herzfeld and Berger.[58] The principal components measured from the MAS spectrum are in very good agreement with those from the non-spinning spectrum, and differ at most by 4 ppm. Since non-spinning spectra generally require much more (twenty times more in this case) spectrometer time to acquire than MAS spectra, all of the data reported in Table 1 were obtained from MAS spectra. Figure 4c shows the ^{13}C MAS spectrum of **1** in frozen SbF_5. The spectrum shows that all the starting material was ionized in this media to form the acetylium ion **1**. This is due to the much stronger Lewis acidity of SbF_5 compared to that of the other metal halides used in this investigation. This and all other spectra reported here were obtained with ^1H decoupling, but ^{19}F decoupling was not used. The lines are slightly broader in Figure 4c compared to Figure 4b, but dipolar coupling to ^{19}F did not otherwise have any noticeable effect on determinations of chemical shift data in SbF_5. Note that the principal components and isotropic shifts for **1** on different media (cf. Table 1) are very similar to each other. Thus,

(65) Schäfer, A.; Horn, H.; Ahlrichs, R. *J. Chem. Phys.* **1992**, *97*, 2571−2577.
(66) ACES II, an ab initio quantum chemical program system. Stanton, J. F.; Gauss, J.; Watts, J. D.; Lauderdale, W. J.; Bartlett, R. J.
(67) The program can be obtained from the authors directly, or via the World Wide Web at http://hawserv80.tamu.edu/hawhomepage/haw1.html.
(68) Reed, A. E.; Weinstock, R. B.; Weinhold, F. *J. Chem. Phys.* **1984**, *83*, 735.
(69) NBO Version 3.1: Glendening, E. D.; Reed, A. E.; Carpenter, J. E.; Weinhold, F.
(70) Mulliken, R. S. *J. Chem. Phys.* **1955**, *23*, 1833−1840.
(71) Mulliken, R. S. *J. Chem. Phys.* **1955**, *23*, 1840−1846.

Table 1. Experimentally Measured Isotropic Chemical Shifts (δ_{iso}), Principal Components (δ_{11}, δ_{22}, and δ_{33}), Chemical Shift Anisotropies (CSA), and Asymmetry Factors (η) for the C_1 Carbons in Acylium Ions **1**−**7**[a]

acylium ion	media	temp, K	δ_{iso}, ppm	CSA, ppm	η	δ_{11}, ppm	δ_{22}, ppm	δ_{33}, ppm
1	$AlBr_3$	113	153	−338	0.00	266	266	−72
	$TaCl_5$	298	154	−348	0.00	271	271	−79
	SbF_5	83	152	−348	0.00	268	268	−80
2	$AlCl_3$	133	154	−329	0.18	284	244	−65
3	$AlBr_3$	133	155	−337	0.13	282	252	−70
4	$AlCl_3$	133	155	−351	0.00	272	272	−79
5	SbF_5	83	146	−331	0.33	292	220	−75
6	SbF_5	83	154	−283	0.24	271	226	−34
7	SbF_5	153	155	−280	0.19	266	231	−31

[a] The standard deviation in the isotropic shifts (δ_{iso}) is 1 ppm. The standard deviation in the principal components (δ_{11}, δ_{22}, and δ_{33}) of the cations **1**, **2**, and **5**−**7** is estimated to be less than 5 ppm. For ions **3** and **4**, the standard deviation is slightly larger, especially in the δ_{11} and δ_{22} components, because of the generally lower S/N ratios in the CP/MAS spectra of these two ions, and is estimated to be less than 10 ppm in δ_{11} and δ_{22} and less than 5 ppm in δ_{33}.

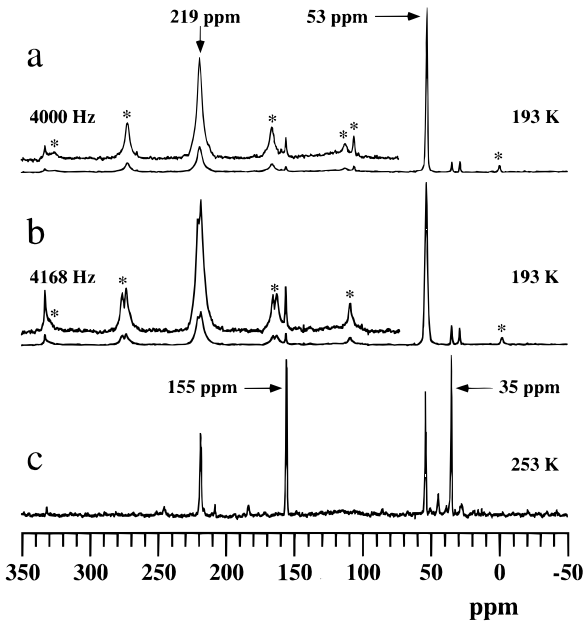

Figure 5. 75.35-MHz ^{13}C Bloch decay spectra acquired after reacting 0.1 equiv of 2-chloro-2-methylpropane-*2*-^{13}C with an excess amount of ^{13}CO on $AlCl_3$ powder at 223 K. Asterisks denote spinning side bands. Figure 5a shows two prominent resonances at 219 and 53 ppm, which were assigned to the donor−acceptor complex between 2,2-dimethylpropionyl-*1*,*2*-$^{13}C_2$ chloride and $AlCl_3$. The rotational resonance condition was achieved when the spinning speed was intentionally set to $^1/_3$ of the frequency difference between the 219- and 53-ppm resonances. The doublet pattern (Figure 5b) in the 219-ppm resonance and its spinning side bands reflects the short internuclear distance, consistent with the formation of a C−C bond. Upon increasing the sample temperature to 298 K, the donor−acceptor complex was converted to **4** (Figure 5c). A small amount of the *tert*-butyl cation was observed at 331 ppm.

whatever effects the differences in Lewis acids have on the chemical shifts of the cations are either nonspecific or too small to be measured by our techniques.

Cations **1**, **2**, **5**, **6**, and **7** were prepared from the corresponding acyl halides. Cations **3** and **4** were prepared by a more novel route; Figure 5 shows the Bloch decay spectra of cation **4**. 2-Chloro-2-methylpropane-*2*-^{13}C (0.1 equiv) was adsorbed on $AlCl_3$ at 223 K, followed by exposure to an excess of ^{13}CO. No CO uptake was observed in control experiments without pre-adsorption of alkyl halide, but in this case the uptake was nearly stoichiometric with respect to halide. The MAS spectra obtained at 223 K showed that the major product was the donor−acceptor complex of 2,2-dimethyl-propionyl-*1*,*2*-$^{13}C_2$ chloride, resulting from the stoichiometric reaction of 2-chloro-2-methylpropane-*2*-^{13}C with ^{13}CO on $AlCl_3$. The ^{13}C-labeled carbons gave isotropic peaks at 219 and 54 ppm for the donor−acceptor complex. A rotational resonance experiment[72] was performed, and the results are shown in Figures 5a and 5b. Since the two peaks were exactly 12 504 Hz apart at the field strength used, the spin speed was set to $^1/_3$ of that peak separation in hertz, i.e., 4168 Hz. At most spinning speeds (e.g., 4000 Hz, Figure 5a), MAS averages the $^{13}C-^{13}C$ dipolar coupling. But, at $^1/_3$ the peak separation, the dipolar coupling was reintroduced, and the 219-ppm peak and its side bands were split into doublets. The figures qualitatively exploit the phenomenon of rotational resonance to demonstrate that the two labeled carbons are fixed close together, as they must be in a chemical bond. This observation of through-space dipolar coupling between the two labels supports the formation of a chemical bond. This sample was then warmed to room temperature, affording cation **4** irreversibly (Figure 5c), and upon reducing the temperature once again, the principal components for C_1 were measured from slow speed spectra (not shown). Note that a small amount of the *tert*-butyl cation can be seen at 331 ppm in each spectrum in Figure 5. Cation **3** was also obtained by this procedure.

We briefly studied acetic acid and acetaldehyde on some of the solid Lewis acids, but we did not observe cation **1** from these precursors.

Experimental Chemical Shift Trends. Experimental values of the ^{13}C principal component data for C_1 of acylium ions **1** through **7** prepared on various solid Lewis acids are compiled in Table 1. In some media the values obtained at 298 K showed some motional averaging (cf. ref 10 for **1**) and are not reported, but only modest cooling sufficed to obtain limiting values. Also included in Table 1 are the CSA and η values calculated from the experimental principal component data. Cation **5** has an isotropic shift of 146 ppm due to the chloro substituent on C_2, but the other cations have isotropic shifts of 154 ± 1 ppm on most media. *Inspection of the principal component data in Table 1 reveals that the negligible variation in isotropic shifts among the acylium ions conceals large variations in the three-dimensional shielding environment.* For example, the C_{3v} symmetry of ions **1** and **4** is reflected in the experimental η values of zero, while the other cations, lacking axial symmetry, have non zero η values. Furthermore, the magnitudes of the chemical shift anisotropies of the benzoylium ions **6** and **7** are ca. 15% smaller than those of ions **1**−**5** due to charge delocalization into the ring. Several of us reported a similar trend in a study of indanyl cations formed in zeolites and associated similar reductions in CSA with resonance delocalization.[73]

Theoretical Results

Geometry and Electronic Structure of 1 and 8−10. We will first discuss the theoretical results for the acetylium ion (**1**) in detail, then touch more briefly on the data for cations **2**−**6**. To highlight the potential computational difficulties associated with **1**, we compare the results to those obtained for methylacetylene (**9**) and acetonitrile (**10**), which are isoelectronic with **1**, and to carbon monoxide (**8**). Selected internal coordinates of the MP2/6-311G* optimized geometries and the NPA partial charges of **1**, **8**, **9**, and **10** are given in Figures 1 and 3.

(72) Levitt, M. H.; Raleigh, D. P.; Creuzet, F.; Griffin, R. G. *J. Chem. Phys.* **1990**, *92*, 6347−6364.

(73) Xu, T.; Haw, J. F. *J. Am. Chem. Soc.* **1994**, *116*, 10188−10195.

Complete geometry information is available as Supporting Information. The NBO and NRT analyses indicate that the C_1 and O in **1** are involved in what is almost a full triple bond, with both the s and p bonds polarized toward oxygen. The p bonds are formed from pure p orbitals, while the s bond is formed by $sp^{1.4}$ hybrids. The lone pair is located on oxygen, and the NPA indicates C_1 carries the positive charge, rather than the oxygen, as the cation is often mistakenly written. The conventional Lewis structure described above is the dominant resonance structure, accounting for 81.6% of the true hybrid. The most important secondary resonance structure involves cumulated double bonds and hyperconjugation:

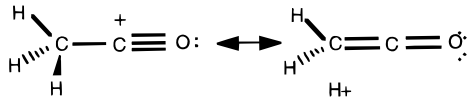

81.6 % 2.7 % (3)

Note that there are three equivalent secondary resonance structures, as indicated above. Although similar resonance structures have been proposed,[3,8] the NRT gives the first quantitative picture of the importance of the possible resonance structures for acylium ions. The NRT analysis indicates a bond order of 2.85 for the C_1-O bond, and 1.15 for the C_1-C_2 bond, consistent with the influence of the secondary resonance structures.

The calculated geometry conforms to the NBO picture of the electronic structure. The theoretical C_1-O distance of 1.127 Å in **1** is consistent with a C_1-O triple bond, and is notably shorter than the calculated lengths of the triple bonds in the related molecules (**8**−**10**). The calculated C_1-O bond length in **1** is long when compared to most of the crystal values (1.08−1.12 Å),[8] although Le Carpentier reports a bond length of 1.138 Å for the salt $[CH_3CO]^+[AlCl_4]^-$.[4] Difficulties in obtaining accurate bond lengths for triple bonds by X-ray crystallography likely contribute to the disagreement between the theoretical and experimental values. Calculations at this level of theory will likely give C−O triple bonds that are slightly too long; our calculated bond length in carbon monoxide is approximately 0.01 Å longer than the experimental value of 1.128 Å.[74] More importantly, the predicted *relative* shortness of the C_1-O bond in **1** compared to **8** agrees with the experimental data. The fact that the C_1-O bond in the acylium cations is noticeably shorter than those found in aldehydes and ketones (1.20 Å) has previously been noted.[8] The calculated C_2-C_1 bond length of 1.439 Å in **1** also compares well to values of 1.385−1.452 Å in acylium crystal structures[8] and is consistent with a somewhat shortened single bond. The slight decrease of the C_2-C_1 bond length from that of a "pure" single bond is consistent with the influence of the secondary resonance structures predicted by the NRT analysis. Higher order correlation, larger basis sets, and consideration of thermal and zero-point effects might give more definitive geometries, but the current theoretical results are within the range of errors reported for the diffraction data, and are sufficiently accurate that meaningful interpretations can be made.

The theoretical bond orders and resonance hybridization in methylacetylene (**10**) are very similar to those of **1**, again indicating a contribution from a cumulated and hyperconjugated resonance structure. The primary Lewis structure, similar to that of **1**, has a weight of 81.8%. Comparison of the geometry of **1** with **10** shows the C_2-C_1 bond length differs by only ≈0.03 Å, again reflecting the resonance structures and increase in bond order. The carbon−carbon triple bond in **10** is almost 0.1 Å longer than the triple bond in **1**.

(74) Herzberg, G. *Spectra of Diatomic Molecules*, 2nd ed.; Princeton, 1959.

Table 2. ^{13}C Isotropic Shifts and Principal Components

molecule	NMR theory level[a]	δ_{iso}, ppm	$\delta_{\perp}$, ppm	$\delta_{\parallel}$, ppm
$[CH_3{}^{13}C{\equiv}O]^+$ (**1**)	RHF/6-31G*	160	280	−79
	RHF/6-311G*	174	304	−86
	RHF/tzp/dz	173	304	−89
	MP2/tzp/dz	154	270	−79
	experiment[b]	152	268	−80
$^{13}C{\equiv}O$ (**8**)	RHF/6-31G*	204	341	−70
	RHF/6-311G*	222	371	−76
	RHF/tzp/dz	222	372	−79
	MP2/tzp/dz	185	315	−74
	experiment[c]	181	293	−42
$CH_3{}^{13}C{\equiv}N$ (**9**)	RHF/6-31G*	119	227	−95
	RHF/6-311G*	131	247	−102
	RHF/tzp/dz	129	247	−105
	MP2/tzp/dz	120	220	−82
	experiment[d]	117	216	−78
$CH_3{}^{13}C{\equiv}CH$ (**10**)	RHF/6-31G*	74	160	−98
	RHF/6-311G*	83	177	−105
	RHF/tzp/dz	82	177	−107
	MP2/tzp/dz	84	168	−84
	experiment[e]	80	166	−93
$CH_3C{\equiv}{}^{13}CH$ (**10**)	RHF/6-31G*	70	134	−58
	RHF/6-311G*	77	147	−63
	RHF/tzp/dz	76	146	−66
	MP2/tzp/dz	67	138	−75
	experiment[e]	69	140	−74

[a] All ab initio geometries are calculated at the MP2/6-311G* level with core electrons frozen. Values are reported relative to those for C in TMS at the same level of theory. Absolute shielding for C in TMS: GIAO-RHF/6-31G*//MP2/6-311G* = 200.8 ppm, GIAO-RHF/6-311G*//MP2/6-311G* = 194.7 ppm, GIAO-RHF/tzp/dz//MP2/6-311G* = 191.8 ppm, GIAO-MP2/tzp/dz//MP2/6-311G* = 199.0 ppm. [b] This report. [c] Gibson, A. A. V.; Scott, T. A.; Fukushima, E. *J. Magn. Reson.* **1977**, *27*, 29−33. Cited values are for solid CO measured at 46 K. [d] Ripmeester, J. A.; Tse, J. S.; Davidson, D. W. *Chem. Phys. Lett.*, **1982**, *86*, 428−433. Cited values were measured in a liquid crystal clathrate (β-quinoline). [e] Beeler, J. B.; Orendt, A. M.; Grant, D. M.; Cutts, P. W.; Michl, J.; Zilm, K. W.; Downing, J. W.; Facelli, J. C.; Schindler, M. S.; Kutzelnigg, W. *J. Am. Chem. Soc.* **1984**, *106*, 7672−7676. These data were reported for a 1:1 (v/v) dilution with argon in the gas phase, frozen for measurement.

Comparison of the electronic structure of **1** with the isoelectronic acetonitrile (**9**) also reveals only small differences. As expected, the dominant Lewis structure of acetonitrile, which accounts for 81.8% of the true hybrid, shows a triple bond between C_1 and N, and a single bond between C_1 and C_2. The C_1-N bond order of 2.87 and the C_2-C_1 bond order of 1.10 are similar to the values in **1**, and also indicate the importance of secondary resonance structures. Interestingly, although the C_1-O bond order in **1** is slightly less than the C_1-N bond order in acetonitrile, the bond length is 0.04 Å shorter. Similarly, the enhanced double bond character of the C_2-C_1 bond in **1** compared to acetonitrile also runs counter to the fact that the calculated bond length in **1** is 0.02 Å shorter than the corresponding bond in acetonitrile. Thus, it appears that the large positive charge on C_1 in **1** gives a much larger ionic component to both bonds, resulting in shorter bond lengths than expected for sp-hybridized carbon. This interpretation agrees with the interpretation of the relative contribution of covalent and ionic bonding from the NRT analysis. Overall, the three isoelectronic species all have similar electronic structures.

NMR Chemical Shifts. In Table 2 we present the GIAO NMR chemical shifts for **1**, **8**, **9**, and **10** predicted by several levels of theory. In each case, the NMR data were calculated at the MP2/6-311G* geometry. These data reveal how both increases in basis set size and the inclusion of electron

correlation affect the theoretical chemical shifts. First, compare the values calculated at GIAO-RHF/6-31G* with those calculated at GIAO-RHF/6-311G*. The additional flexibility provided by the 6-311G* basis set has a substantial effect on the predicted isotropic shift and $\delta_\perp$, resulting in values that move downfield by as much as 36 ppm. In contrast, the values of $\delta_\parallel$ are not affected. Interestingly, the GIAO-RHF/6-31G* results are closer to experiment than those obtained at GIAO-RHF/6-311G*. The substantial differences in the values predicted by the two basis sets indicate a strong sensitivity to basis set flexibility and that the agreement at the GIAO-RHF/6-31G* level is due to a fortuitous cancellation of errors. The need for a triple-ζ or better description of heavy atoms in NMR calculations was noted previously.[29] Not surprisingly, the NMR values calculated at GIAO-RHF/6-311G* agree closely with those obtained at the GIAO-RHF level using the tzp/dz basis sets of Ahlrichs. The differences between the results from the two GIAO-RHF calculations with the more flexible basis sets are at most 4 ppm, although the GIAO-RHF/tzp/dz scheme gives values that are always in equal or worse agreement with experiment than the GIAO-RHF/6-311G* results.

As expected, the inclusion of electron correlation has a substantial effect on the calculated NMR data. Comparing the GIAO-RHF/tzp/dz and GIAO-MP2/tzp/dz results we obtain differences as large as 57 ppm in the $\delta_\perp$ values, while the calculated isotropic and $\delta_\parallel$ values are again much less sensitive. These results are consistent with the calculations referenced earlier, which indicated that electron correlation was important in obtaining agreement with experimental data for cations and molecules with double and triple bonds. The agreement between our calculated GIAO-MP2 isotropic chemical shifts for molecules **8**, **9**, and **10** and experimental data is very good; in most cases the values differ by less than 4 ppm. The principal components are also in good agreement with the experimental values, with the exception of the $\delta_\perp$ value of **8**. At higher levels of theory with larger basis sets, the agreement between experiment and the isotropic chemical shift calculation is only slightly better. At SDQ-MP4,[32] the difference between theory and experiment in the isotropic chemical shift is only 3.5 ppm. When CCSD was used in the shift calculations, the difference was reduced to 0.2 ppm.[33] Those studies did not report the principal component data. Note that the calculated data should ideally be compared to the results of gas-phase experiments. The good agreement between the GIAO-MP2 values and the solid-phase measurements suggests the interactions in the crystal are small or do not influence the isotropic chemical shift of C_1.

More accurate representations of electron correlation in the NMR calculations (i.e. MP4 or CCSD)[32,33] might lead to further improvements in the agreement with experiment. Such calculations would be very expensive and possibly intractable for the larger cations included in this study.

Geometric and Electronic Structure of 2−7. Selected internal coordinates and charges of the MP2/6-311G* optimized structures of the six additional acylium ions (**2**−**7**) in this investigation are also given in Figures 1 and 2. We first consider the acylium ions **1**−**5**. The slight changes in the C_1−O and C_2−C_1 bond lengths across the series of molecules reflect the changes in charge distribution as the size of the alkyl R-groups increase. Thus, as we move from R = CH_3 in **1** to R = $(CH_3)_3C$ in **4**, the C_1−O bond length increases from 1.127 to 1.132 Å, while the NRT C_1−O bond order decreases from 2.850 to 2.841. The same effect is seen in the C_2−C_1 bond, which lengthens from 1.439 to 1.446 Å between **1** and **4** as the bond order decreases from 1.150 to 1.062. The positive charge on C_1 remains relatively constant across the series, but the negative charge on C_2 decreases substantially, from −0.828 |e| in **1** to −0.184 |e| in **4**, while the negative charge on O increases from −0.107 to −0.148 |e|. The results indicate that increasing the number of methyl groups bonded to C_1 causes charge on C_1 to be depleted, while the charge on the methyl carbons increases. This may account for the decrease in the C_2−C_1 bond order, and the lengthening of the bond.

The electron withdrawing nature of the chloro substituent in acylium cation **5** results in decreased electron density on C_2 and a decrease in the C_2−C_1 bond order (2.838). However, the C_2−C_1 bond (1.120 Å) is noticeably longer than in **1**−**4**, possibly due to steric repulsion between Cl and C_1. The expected dominant resonance structure has a weight of 76.9%. While hyperconjugated resonance structures (each contributing 3.5% or less to the total resonance hybrid) similar to those for **1**−**4** are also indicated by the NRT, an interesting Lewis structure for **5** involves a bond between C_1 and Cl:

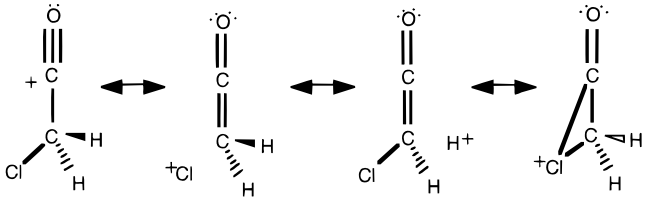

76.9 % 3.5 % 3.2 % (2) 3.5 %

Donation of charge from Cl to C_1 would be consistent with increased shielding and the noticably upfield NMR chemical shift for C_1 in **5** compared to the acyliums. However, the very small contribution (weight = 3.5%) this resonance structure makes to the overall hybrid and the fact that the NPA charge on C_1 in **5** (−0.592) is very similar to that of C_1 in **2** (−0.616) argue against this resonance structure having a noticable effect on the chemical shift.

The electronic structures of two benzoylium ions (**6**, **7**) are very similar to one another, but quite different from the alkyl series. There is a substantial contribution from secondary resonance structures, with the two conventional Kekulé structures having a combined weight of only 43.4% for **6** and 37.1% for **7**. The most important secondary resonance structure for **6**, with a weight of 7.8%, places a lone pair on C_2. In addition, a large number of cumulated and hyperconjugated resonance structures are possible:

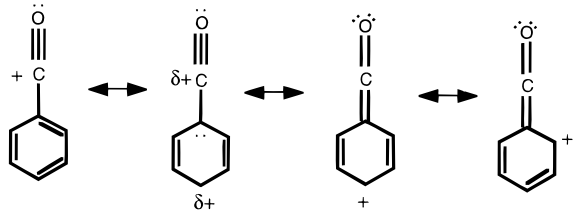

21.7 % (2) 7.8 % 3.5 % 3.5 % (2)

The importance of the secondary resonance structures is evident in the shorter bonds (1.392 Å in **6** and 1.386 Å in **7**) between the *ortho* and *meta* carbons relative to the other carbon−carbon bonds of the ring. A shortening of the ortho−meta bonds is also observed experimentally; they are 1.363 Å in the crystal structure of a similar acylium ion ($[p\text{-}CH_3\text{-}C_6H_6CO]^+[SbCl_6]^-$).[4] The experimental C_2−C_1 bond length of 1.396 Å in the same compound is also in good agreement with the optimized geometries of the benzoylium ions. The significant delocalization of charge (and the substantial contributions of secondary resonance structures) in the phenyl compounds certainly con-

Table 3. GIAO-MP2/tzp/dz ^{13}C Isotropic Shifts and Principal Components of Acylium ions **2**−**7**[a]

ion	$\Delta\delta_{iso}$, ppm	ΔCSA, ppm	η	$\Delta\delta_{11}$, ppm	$\Delta\delta_{22}$, ppm	$\Delta\delta_{33}$, ppm
1	2	−1	0.00	2	2	1
2	2	−25	0.02	−7	27	−15
3	3	−20	0.03	−2	21	−10
4	4	−9	0.00	7	7	−2
5	4	−12	0.01	−27	43	−4
6	6	−2	0.12	−4	17	4
7	5	0	0.14	1	10	5

[a] Chemical shifts and CSA are reported as deviation from experiment (theoretical value − experimental value).

tributes to the unusually short C_2-C_1 bond length. Also consistent with the influence of the secondary resonance structures, the optimized C_1-O bond lengths in **6** and **7** are slightly longer than those in the aliphatic molecules. This effect is not observed in the crystal data,[8] but is likely outside the accuracy of the experimental measurement. In all cases, the optimized acylium cations have a linear arrangement for C_2-C_1-O. The crystal structure data support these results, as the reported bond angles range from 175.7° to 180.0°.[8]

NMR Chemical Shifts for 2−7. The GIAO-MP2/tzp/dz chemical shift tensors for acylium ions **1**−**7** are shown in Table 3, reported as the deviation from the experimental values. The predicted isotropic values are in excellent agreement with the experimental data; the largest difference is 6 ppm. The theoretical values are consistently shifted downfield from the experimental result. Although the theoretical principal components are generally also in good agreement with experiment, there are some noticeable errors, the largest of which is the 43 ppm downfield prediction for δ_{22} in **5**. The only trend in the deviation between the theoretical and experimental values of the principal components is that the theoretical values of δ_{22} are all downfield from experiment.

The most notable disagreement between the theoretical and experimental data appears in the asymmetry parameter. Theory predicts values close to zero for **1** and **4**, consistent with the experiment and required by molecular symmetry. However, the asymmetry is also close to zero for **2**, **3**, and **5**, while the experimental values range from 0.13 to 0.33.

Orientation of the Chemical Shift Tensors. Figure 6 shows the orientation of the principal components of the chemical shift tensor for ions **1**, **5**, and **6**. For acylium **1** (Figure 6a) δ_{33} lies along the C_1-O bond axis, and δ_{11} and δ_{22} lie in a plane perpendicular to the C_1-O bond. Due to the C_{3v} symmetry of this atom, δ_{11} and δ_{22} can have any orientation in the plane perpendicular to the C_1-O bond, provided that they are perpendicular to one another. For consistency with the other shown cases, the principal components of **1** are shown in Figure 7 with δ_{22} lying in one of the three C_s planes of the molecule, and thus δ_{11} lies out of the page. For all the acylium cations studied here, δ_{33} lies along the C_1-O bond. Although the magnitudes of the tensor components of **2**−**4** are slightly different from that of **1**, the orientations are the same**.** In the chlorine-containing compound (**5**, Figure 6b) δ_{33} lies 0.5° off of the C_1-O bond axis, in the $Cl-C_2-C_1$ plane, angled toward the Cl atom. Somewhat opposite of the case for acyliums **1**-**4**, in **5** δ_{11} lies in the $Cl-C_2-C_1$ plane, whereas δ_{22} is perpendicular to that plane. In the phenyl-substituted acyliums (**6** and **7**) δ_{11} is perpendicular to the plane of the ring, whereas δ_{22} is in the plane of the ring, perpendicular to the C_1-O bond. The orientation of the principal components for **6** is shown in Figure 6c.

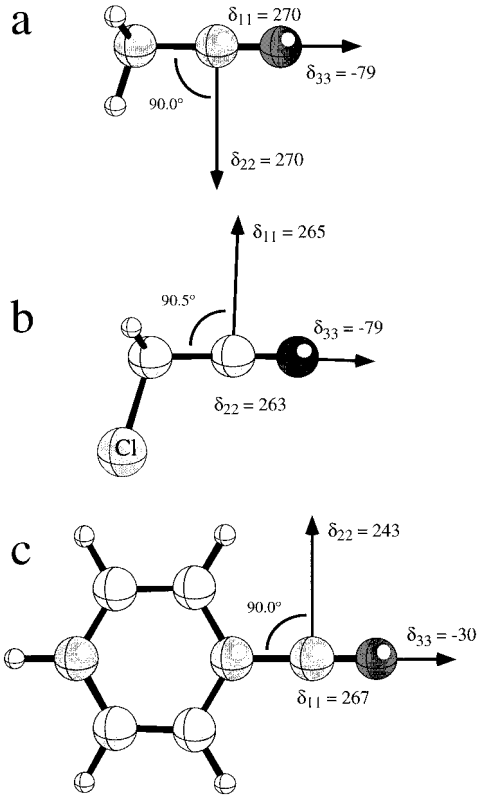

Figure 6. Orientations of the GIAO-MP2/tzp/dz chemical shift tensors for acylium ions **1** (a), **5** (b), and **6** (c).

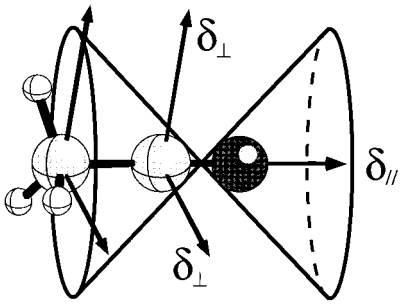

Figure 7. Qualitative description of magnetic anisotropy of **1** based on a semiclassical model.

Discussion

An interesting aspect of the current work is the consideration of the effect the media has on the acylium cations. The theoretical calculations represent isolated, gas-phase cations. The close correspondence between the theoretical and experimental results suggests that the acylium ions do not strongly interact with the metal halide powder, or that the chemical shift is relatively unaffected by any such interactions. Indeed, the crystal structures of acylium ions determined in strong Lewis acids have long distances (2.5−3.0 Å) between the carbenium carbon and the nearest halides, indicating no *direct* interaction between the cations and anions. However, a recent ab initio molecular orbital study of CH_3CO^+ complexed to $AlCl_4^-$ and $Al_2Cl_7^-$ by Jasien[75] suggests a much more pronounced interaction between the cation and the anions, resulting in a bent C_2-C_1-O bond angle (166.9−173.2° for ion pairs). Further experimental study of **1** gave an isotropic chemical shift for C_2 of 12.1 ppm, in notable disagreement with the GIAO-MP2/tzp/dz value of 4.6 ppm. To investigate the sensitivity of the theoretical chemical shift to changes in geometry we calculated

(75) Jasien, P. G. *J. Phys. Chem.* **1995**, *99*, 6502−6508.

Table 4. GIAO-MP2/tzp/dz ^{13}C Isotropic Chemical Shifts for C_1 and C_2 for Various Values of the C_2-C_1-O Bond Angle in **1**

C_2-C1-O bond angle	δ_{iso} C1	δ_{iso} C2
175	153.6	5.4
170	153.7	6.1
165	154.0	7.3
155	155.0	11.4
145	156.6	17.6

the NMR data for several different geometries of **1**. We first considered changing the C_2-C_1-O bond angle across a range from 175° to 145°. The rest of the internal coordinates of the molecules were optimized while the C_2-C_1-O bond angle was held fixed. The results are shown in Table 4. Surprisingly, the chemical shift of C_1 is insensitive to variation of the bond angle, and even values of the bond angle as small as 145° produce only a 3-ppm change in the C_1 chemical shift. However, the chemical shift of the methyl carbon (C_2) is highly responsive to the degree to which the bond is bent; at 145° the chemical shift of C_1 is 17.6 ppm, 12.2 ppm downfield from the value in the linear molecule. We might consider that better agreement with experiment could be obtained by assuming that the cation interacts with the Lewis acid in a fashion similar to that proposed by Jasien,[75] with resultant changes in the C_2-C_1-O bond angle. However, the linear geometries in the crystal structures seem to argue against this explanation.

Alternately, changes in the bond lengths of **1** also affect the chemical shift and may be responsible for the discrepancy between the theoretical and experimental values for C_2. For example, optimization of **1** with the C_2-C_1-O bond angle constrained to 170.0° gives an increase in the C_2-C_1 bond length of 0.0016 Å, while the strong C_1-O bond length lengthens by only 0.0003 Å. To determine how changes in bond length alone affect the calculated results, we optimized the C_{3v} geometry of **1** with the C_2-C_1 bond length increased by 0.05 Å. This calculation predicts an isotropic shift of 153.7 ppm for C_1 and 10.8 ppm for C_2. Similar calculations with the C_2-C_1 bond length decreased by 0.05 Å gave isotropic chemical shifts of 153.5 for C_1 and 5.1 for C_2. We see that C_1 is again relatively unaffected by either geometry change, while the isotropic value for C_2 is shifted considerably downfield by the increase in bond length. While such changes in internal coordinates may contribute to the discrepancy between the theoretical and experimental chemical shift for C_1, this matter is currently unresolved.

A final possible contribution to the discrepancy is weak dipolar coupling to ^{35}Cl and ^{37}Cl. Such coupling could reasonably modify the side-band intensities in a way that maps into a few ppm error in calculated chemical shift principal components. Our intuition is that this contribution is smaller than imperfections in the calculated geometries or shifts.

The acylium ions studied have isotropic chemical shifts of approximately 154 ppm, which is upfield of most simple carbenium ions. In the parlance of qualitative chemical shift interpretation, this (as well as the upfield shift for the methyl carbon of **1**) reflects the magnetic anisotropy of the triple bond. Figure 7 shows the qualitative picture of shielding due to magnetic anisotropy for **1**; the conical volumes denote the most shielded regions according to the qualitative treatment, and the chemical shift tensors obtained at GIAO-MP2/tzp/dz are inscribed onto the structure for both C_1 and the methyl carbon. A careful examination of Figures 1 and 3 and the data in Table 2 shows that the familiar concept of magnetic anisotropy is a useful way to rationalize the orientation and values of the principal components of the chemical shift for carbons near triple bonds. The δ_{33} components are shifted very far upfield; for comparison, the δ_{33} for acetone is 79 ppm.[42] It can be easily seen that the magnetic anisotropy has a greater effect on the $\delta_{||}$ (δ_{33}) component and less effect on $\delta_{\perp}$ (δ_{11} and δ_{22}). These effects are also apparent in the methyl carbon tensor, although the anisotropy is, as expected, much smaller. Both the theoretical and experimental data for acylium cations **2**−**7** show the same trend (a strong upfield shift for δ_{33} and less effect on δ_{11} and δ_{22}). Thus, all the chemical shift tensors of all the molecules studied in this work show the effects of magnetic anisotropy.

Conclusion

We have greatly extended our initial investigation of **1** on $AlCl_3$ powder to include a variety of acylium ions and solid Lewis acid media. In doing so we have also obtained the ^{13}C chemical shift tensors for these cations. Two of these cations were prepared by the reaction of an alkyl halide and CO (Koch−Haff reaction). The work suggests the potential of using Lewis acid powders as heterogeneous catalysts.

The isotropic chemical shifts and chemical shift tensors calculated at the highest level of theory (GIAO-MP2/tzp/dz) are in excellent agreement with the experimental values. Consistent with prior studies, it appears that electron correlation is required in order to obtain accurate results for cationic and triply-bonded molecules. The effect of electron correlation enters both in the determination of the optimized geometries and in the GIAO calculation. Although NMR data calculated at the GIAO-RHF level using the MP2/6-311G* geometries are sometimes fortuitously accurate, as the GIAO-RHF/6-31G* data presented here indicate, the evidence is strongly suggestive that correlated GIAO calculations are required in these difficult cases.

The increasing improvements in computer speed will allow the routine calculation of ab initio chemical shift data with more accurate descriptions of electron correlation and larger basis sets. Consequently, more accurate results will be achieved with reasonable computation time. The chemical shift parameters were recently calculated for several carbenium ions, including the benzenium[29] and allyl cation.[76] We believe that further progress toward the measurement of chemical shift tensors for organic molecules, especially for unstable carbenium ions, can make use of high level ab initio calculations combined with necessary confirmations from experiments.

Acknowledgment. Work at Texas A&M University was supported by the National Science Foundation (CHE-9528959) and U.S. Department of Energy (DOE) (Grant No. DE-FG03-93ER14354). J.B.N. is supported by the Office of Basic Energy Sciences of DOE and by Laboratory Directed Research and Development funding provided by Pacific Northwest National Laboratory (PNNL). Computer resources were provided by the Scientific Computing Staff, Office of Energy Research, at the National Energy Research Supercomputer Center (NERSC), Livermore, CA, and the Texas A&M University Supercomputing Facility. PNNL is a multiprogram national laboratory operated by Battelle Memorial Institute for the DOE under Contract DE-AC06−76RLO1830.

Supporting Information Available: A listing of the final optimized geometries using MP2(fc)/6-311G* (4 pages). See any current masthead page for ordering and Internet access instructions.

JA962944N

(76) Buzek, P.; Schleyer, P. v. R.; Vancik, H.; Mihalic, Z.; Gauss, J. *Angew. Chem., Int. Ed. Engl.* **1994**, *33*, 448−451.